Canadian Journal of Microbiology

Research Article

Successional stages and inferred functional profiles of bacterial communities under biocrusts in post-mining ecosystems of Western Boreal Quebec

Gabriel F. Peñaloza-Bojacá[a,b], **Laura Hjartarson**[a,b,c,d], **Marta Alonso-Garcia**[a,b,e], **Juan Carlos Villarreal Aguilar**[a,b,c], **Line Rochefort**[c,d,f], **and Mélina Guêné-Nanchen**[c,d,f]

[a]Biology Department, Université Laval, Québec, QC, Canada; [b]Institute of Integrative Biology and Systems (IBIS), Université Laval, Québec, QC, Canada; [c]Centre for Northern Studies (CEN), Université Laval, Québec, QC, Canada; [d]Peatland Ecology Research Group, Université Laval, Québec, QC, Canada; [e]Departamento de Biología Vegetal (Botánica), Universidad de Murcia, Murcia, Región de Murcia, España; [f]Plant Science Department, Université Laval, Québec, QC, Canada

Corresponding authors: **Gabriel F. Peñaloza-Bojacá** (email: gpenaloza.bojaca@gmail.com); **Mélina Guêné-Nanchen** (email: melina.guene-nanchen.1@ulaval.ca)

Abstract

Mine tailings are inhospitable to plant establishment because of substrate instability, nutrient limitation, heavy metals, and temperature fluctuations at the soil surface. Biological soil crusts (biocrusts) and their associated microbial communities can initiate primary succession and facilitate plant–soil interactions, thereby supporting ecosystem recovery. Here, we characterized soil bacterial communities beneath biocrusts along a successional gradient in abandoned and rehabilitated molybdenum–bismuth mine tailings in Western Boreal Quebec. We collected 125 soil samples from bare soil, cyanobacterial-, chlorolichen-, and bryophyte-dominated biocrusts, as well as from a mixed bryophyte–lichen cover layer. Bacterial communities were assessed using amplicon sequencing (16S rRNA and nifH genes) and linked to soil physicochemical properties to infer functional potential. Soil pH, electrical-conductivity, and sulfur content were associated with bacterial diversity (distance-based redundancy analysis, $R^2 = 0.20$, $p < 0.01$). Rehabilitated sites exhibited moderate relative abundances of Proteobacteria (6.9%), whereas Actinobacteriota prevailed in nutrient-poor abandoned sites (17.1%), consistent with oligotrophic adaptation. Additionally, functional potential from chemoheterotrophy in later stages was associated with sulfur-oxidation (Spearman's $\rho = 0.6$, $p < 0.05$), with anoxygenic photoautotrophs potentially contributing to sulfur oxidation. Overall, our study indicates that bacterial communities may contribute to soil stabilization and could serve as key bioindicators of restoration success.

Key words: diazotrophic bacteria, boreal forest, primary succession, mine tailings, 16S gene, soil physicochemical properties

Introduction

Mine tailings, the waste materials generated during the mining process, are often inhospitable to plant establishment due to substrate instability and extreme temperature fluctuations at the soil surface (Guittonny and Bussière 2020). These tailings typically exhibit low nutrient availability, with essential elements such as fixed nitrogen and soluble phosphorus being scarce (Sun et al. 2024). Additionally, sulfur compounds and metal(loid)s are present in high concentrations (Gadd 2010; Sun et al. 2020, 2024). These multiple environmental stresses significantly hinder the establishment of organisms in mine tailings (Weber et al. 2022; Sun et al. 2024). In such extreme environments, where resource acquisition is severely limited, microbial and plant-microbe facilitation—such as stress-triggered strengthening of nutrient-cycling microbial networks—can play a vital role in ecosystem recovery (Hammarlund and Harcombe 2019; Hernandez et al. 2021; Mandakovic et al. 2023).

The natural vegetative progression that occurs on mine tailings is primary succession, as these substrates lack organic material and plant propagules (Weber et al. 2022). The first organisms colonizing these surfaces are heterotrophic noncyanobacterial diazotrophs, organisms that contribute to nitrogen fixation (Pepe-Ranney et al. 2016) and biological soil crusts (biocrusts) (Weber et al. 2022; Lan et al. 2024), which are known for their strong adaptability in degraded environments (Cowden et al. 2022; Liao et al. 2024). Biocrusts cover approximately 12% of Earth's land surface and are often referred to as the "living skin" of the soil (Lan et al. 2024; Sun et al. 2024). During primary succession, biocrusts play a key role in stabilizing the substrate (e.g., contribute to soil aggregation, carbon and nitrogen accumulation, and reduce soil

erosion) and facilitating the establishment of plant species (Eldridge and Greene 1994; Harris 2009; Deng et al. 2020; Watson et al. 2022; Geng et al. 2023; Chowaniec et al. 2024).

Biocrusts are composed of photoautotrophic (e.g., cyanobacteria, algae, lichens, bryophytes) and heterotrophic (e.g., bacteria, fungi, archaea) organisms, which bind together with soil particles to form a stable surface layer (Chamizo et al. 2012; Weber et al. 2022). These can be classified based on their dominant photoautotrophic organisms: cyanobacterial-dominated biocrusts colonize in the early stages of succession (Geng et al. 2023; Duan et al. 2024), consist of algae and cyanobacteria, which have specialized adaptations such as drought resistance, tolerance to extreme temperatures and pH, and relatively rapid growth (Maier et al. 2018; Sun et al. 2024). They contribute to soil aggregation, carbon and nitrogen accumulation, and reduced soil erosion (Eldridge and Greene 1994; Deng et al. 2020; Chowaniec et al. 2024). Later, successional stages are characterized by chlorolichens- and bryophytes-dominated biocrusts (Lan et al. 2013), which exhibit higher photosynthetic efficiency, enhance soil improvement, and increase carbon productivity (Chowaniec et al. 2024). In addition, serving as the ground layer in many forest types (e.g., Acadian, Picea, and mixed wood forests), lichens and mosses stabilize the soil, prevent nutrient runoff, and provide habitat for other plants, mesofauna and microbial species (Smith et al. 2015; Haughian and Burton 2018; Maier et al. 2018; Vitt et al. 2019; Rinehart et al. 2022). These mature biocrusts are also more resistant to erosion, desiccation, and harsh physicochemical conditions, making them crucial for ecological restoration processes (Maier et al. 2018; Gao et al. 2020; Sun et al. 2024).

Additionally, bacterial communities beneath biocrusts vary according to the dominant photoautotrophs at the surface, as each group provides distinct ecosystem functions (Maier et al. 2018). These functions regulate key soil attributes and biogeochemical cycles, including nutrient availability, carbon cycling, and microbial activity, which are crucial for ecosystem sustainability in degraded environments (Chamizo et al. 2012; Eldridge et al. 2020; Liao et al. 2024; Sun et al. 2024). For example, bacterial communities beneath biocrusts can influence the total soil organic carbon content, which plays a fundamental role in maintaining soil fertility. Soil organic carbon helps regulating water retention and the microclimate, and supports the decomposition of organic matter, all of which are crucial for ecosystem productivity (Dou et al. 2024). In addition to carbon cycling, biocrusts are also significant contributors to global nitrogen inputs, fixing an estimated 30% of the biologically fixed nitrogen annually (Elbert et al. 2012). Biological nitrogen fixation (BNF) in biocrusts is carried out by a variety of organisms, including moss-associated bacteria, lichens with cyanobacterial photobionts, free-living cyanobacteria, and other diazotrophs (Barger et al. 2016; Salazar et al. 2022; Escolástico-Ortiz et al. 2023). Among these, moss-associated diazotrophic bacteria are particularly noteworthy, as they use the nitrogenase enzyme to convert atmospheric nitrogen (N_2) into bioavailable ammonia (NH_3), contributing significantly to nutrient cycling in northern ecosystems. For instance, BNF by moss–bacteria symbioses contributes approximately 1.5–2.0 kg N ha^{-1} $year^{-1}$ in boreal forests and up to 5 kg N ha^{-1} $year^{-1}$ in the arctic tundra (DeLuca et al. 2002; Rousk et al. 2013; Escolástico-Ortiz et al. 2023).

The objective of this study is to characterize the composition of soil bacterial communities under biocrusts throughout the ecological succession process in abandoned molybdenum–bismuth mine tailings in the boreal forest of Western Boreal Quebec, Canada. We hypothesize that (i) soil physicochemical properties differ between early (cyanobacterial-dominated), and late (chlorolichen-, bryophyte-dominated) successional stages and influence the composition of bacterial communities in soil beneath biocrusts; (ii) soil under biocrusts exhibits differences in bacterial diversity, community composition, and predicted functional potential as succession progresses.

Materials and methods

Study site and sampling design

The study site is in the Preissac municipality in the Abitibi Regional County Municipality of Quebec, Canada. Mean annual temperature of the region is 16.7 °C and −17.9 °C in July and January, respectively (Government of Canada 2022). Mean annual rainfall and mean annual snowfall of the region are 705 and 281 mm, respectively (Government of Canada 2022). The region is situated within the continuous boreal forest, and the sampling sites were surrounded by a black spruce and feathermoss forest. The Preissac mine was exploited for molybdenum and bismuth between 1962 and 1971 and subsequently abandoned (CANMET 1976). In 1992, rehabilitation efforts were undertaken at Site A (rehabilitated site; 48.3330°N, −78.3912°W), which included planting *Picea mariana* (Mill.) Britton, Sterns & Poggenburg, and applying a booster fertilizer in 1995. No restoration efforts were carried out at Site B (abandoned site; 48.3476°N, −78.3948°W), located approximately 1.5 km north of Site A (Fig. 1). These tailings may contain remnants of pyrite and molybdenum, potentially leading to acid mine drainage, leaching, and contamination by dioxins and furans in the ecosystem (Boily 1995; CIM 2023).

At the abandoned site, five 1 m^2 plots were established for each of the ground cover types (bare soil, cyanobacterial-dominated, chlorolichens-dominated, bryophytes-dominated biocrusts), for a total of 20 plots. Where the bryophytes-dominated biocrusts were primarily composed of mosses from the genera *Polytrichum* and *Bryum*, whereas chlorolichens-dominated biocrusts were characterized by lichens from the genus *Cladonia*. Each plot was treated as a biological replicate and was located at least 10 m from adjacent plots to minimize spatial autocorrelation of soil physicochemical properties and microbial communities (Geng et al. 2023; Duan et al. 2024; Sun et al. 2024), while ensuring adequate spatial coverage of the tailings area. Within each plot, five independent soil samples were collected as subsamples to capture micro-scale heterogeneity within the same biological replicate, and each subsample was processed individually for DNA sequencing (25 samples per ground cover type; 100 total). At the rehabilitated

Fig. 1. Study sites and ground cover under biological soil crust and cover layer in post-mining ecosystems of Western Boreal Quebec. (A) Preissac mine site in Western Boreal Quebec; (B) abandoned site (UNR); (C) rehabilitated site (REH). From abandoned mine: (D) UNR-bare soil; (E) UNR-cyanobacterial-dominated biocrusts; (F) UNR-chlorolichens-dominated biocrusts; (G) UNR-bryophytes-dominated biocrusts. From rehabilitated site (H) REH-bryophyte/lichen cover layer. Arrows indicate representative organism of each biocrust and cover layer.

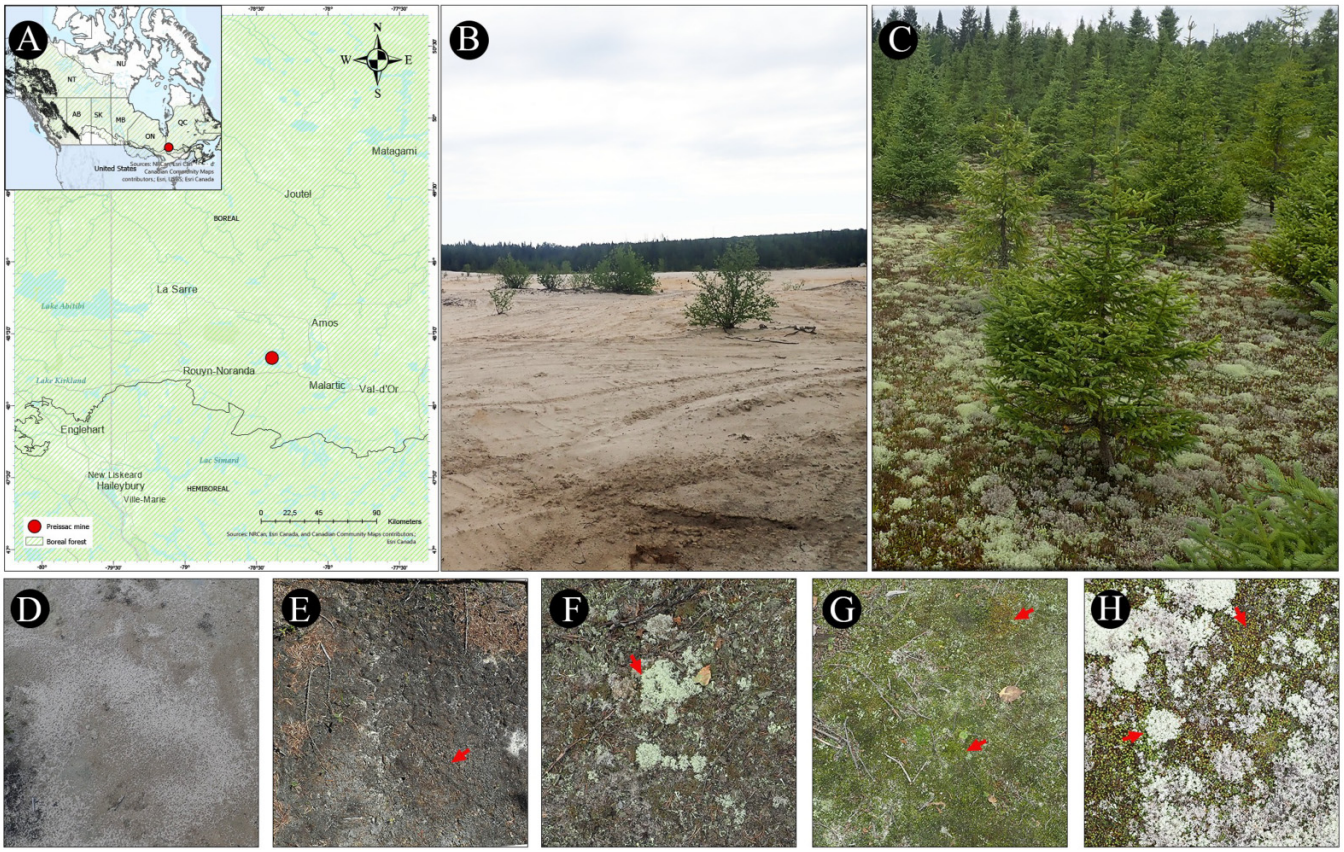

site, five 1 m^2 plots were established in the only ground cover present (bryophyte/lichen), and five subsamples were collected within each plot (25 samples). Because only one biocrust type occurred at this site (bryophyte/lichen cover layer with *Polytrichum* spp. and *Cladonia* spp.), the design is inherently unbalanced between sites. In both sites, a separate composite soil sample was collected per plot for physicochemical analyses (25 samples in total). Soil samples were collected from just below the biocrust or ground-layer surface (≤5 cm), over 2 days in August 2021, using sterile equipment, placed in Eppendorf tubes (DNA samples) or sterile bags (physicochemical samples), stored on ice, and frozen at −20 °C until analysis.

Soil sample processing

Soil pH and electrical conductivity (EC; $\mu S \cdot cm^{-1}$) were measured using a water dilution of 1:1 with an AB150 pH meter (Fisher Scientific, Hampton, New Hampshire, USA) and an Orion Model 122 conductivity meter (Thermo Electron Corporation, Waltham, MA, U.S.A.), respectively. Percent organic matter (perOM) was measured using the loss of ignition method. Soil samples were dried at 105 °C for 24 h, weighed, then ignited in a muffle furnace at 550 °C for 3 h 20 min, with intermediate and final weights recorded after cooling in a desiccator. Percent total carbon (C), nitrogen (N), and sulfur (S) were measured using the LECO TruMac® CNS analyzer. Potassium (K) and magnesium (Mg) were measured by argon plasma ionizing source mass spectrometry (CEAEQ 2014). Phosphorus (P) was measured by the Bray test (Bray and Kurtz 1945) using an inductively coupled plasma optical emission spectrometer (ICP-OES; Agilent, model 5110). Ammonium (NH_4) was extracted according to the standard QuikChem® method 10-107-06-2-B "Ammonia in surface water, wastewater" in FIA QuikChem 8500 Serie two from Lachat (Keeney and Nelson 1982). All analyses were carried out at the Quebec Environmental Analysis Expertise Centre.

DNA extraction, PCR amplification, and high–throughput sequencing

Genomic DNA was extracted using the NucleoSpin Soil DNA Extraction Kit (Takara Bio USA, Inc.). The V3–V4 region of the bacterial 16S rRNA gene was amplified using primers 341F and 805R (Muyzer et al. 1993). The nifH gene was amplified using primers Ueda19F and R6 (Ueda et al. 1995; Marusina et al. 2001). PCR programs for 16S rRNA gene and nifH gene followed (Escolástico-Ortiz et al. 2023). In both

cases, all PCR products were verified on 1.7% agarose gels, and negative extraction and no-template controls were included, showing no evidence of contamination. Samples were pooled in equimolar ratio and sequenced following Bell-Doyon et al. (2020, 2022) and Escolástico-Ortiz et al. (2023) on Illumina MiSeq 300-bp paired-end run (600 cycle, v3 kit), included as 25% of the run, at the Platform of genomic analysis of the Institute of Integrative Biology and Systems, Université Laval, Québec, Canada.

Amplicon sequence data processing

Statistical analyses were conducted using R v.4.4.0 (R Core Team 2024). For 16S rRNA gene analyses, the *DADA2* v.1.26 pipeline was used to assign amplicon sequence variants (ASVs; Callahan et al. 2016). Raw reads were trimmed and filtered, and forward and reverse reads were merged. Sequences with less than 400 base pairs and chimeras were removed. Taxonomy was assigned using the *SILVA* v.138.1 database (Quast et al. 2012; Yilmaz et al. 2014). ASVs corresponding to chloroplast and mitochondrial sequences were removed. Contaminants were identified and removed using the package *Decontam* v.1.14 (Davis et al. 2018). A prevalence threshold was determined to keep ASV present in at least 5% of samples (Callahan et al. 2016, 2017). In addition, for nifH data analyses, we used *DADA2* to quality-check, filter, and trim sequences with the same parameters as for 16S rRNA gene but using a truncation length of 270 bp for the forward and 210 for the reverse complement. Chimeric sequences were removed, and taxonomy was assigned to the ASV table using the data bases nifH *dada2* v.2.0.5 (Moynihan and Reeder 2023). Finally, chloroplast and eukaryotic sequences were removed and only sequences assigned to the Bacteria and Archaea were kept. Sequence data were deposited in the National Center for Biotechnology Information (NCBI) Sequence Read Archive under the BioProject number PRJNA1225235.

Characterization of bacterial community

To compare the bacterial composition in the soil beneath different biocrusts and cover types, we transformed the 16S rRNA and nifH genes data taxa counts to relative abundances using the package *phyloseq* v.1.48 (McMurdie and Holmes 2013). The relative abundance of each phylum, order, and 20 most abundant families was compared between each biocrusts and cover types. We normalized the taxon table to compare alpha diversity between habitats using the relative abundance and multiplying it by a constant of 1000 to obtain count data (McKnight et al. 2019). Using the normalized data, Shannon–Wiener, Simpson, and Pielou indexes were calculated to determine alpha diversity of the bacterial communities from soil below each biocrusts and cover types. Faith's phylogenetic diversity was calculated using a phylogenetic tree constructed with aligned sequences using a neighbour-joining algorithm (Faith 1992). First, we aligned sequences in *decipher* v.2.22 (Wright 2016) with default settings. Then, a phylogenetic tree was constructed using a neighbour-joining algorithm with a GTR + GAMMA model in *phangorn* v.2.8.1 (Schliep 2011) for both 16S and nifH data. Finally, we used the package *picante* v.1.8.2 (Kembel et al. 2010) to compute the phylogenetic diversity using the normalized data and the unrooted maximum-likelihood tree. To examine differences in bacterial composition in soil beneath biocrusts and cover types, we first assessed data normality using the Shapiro–Wilk test. Next, to normally and non-normally distributed data, we used the Kruskal–Wallis and a post hoc Dunn's test for multiple comparisons. All statistical analyses were conducted on *R* v.4.4.0 (R Core Team 2024).

To assess beta diversity in the 16S and nifH data, we computed Generalized UniFrac (GUniFrac) distances using the phyloseq object containing normalized abundance data and a phylogenetic tree (*GUniFrac* v.1.8; Chen et al. 2012). We then used permutational multivariate analysis of variance (PERMANOVA) to test for significant differences between sites (abandoned vs. rehabilitated) and between biocrusts (cyanobacterial-dominated, chlorolichens-dominated, bryophytes-dominated biocrusts) and cover type (bare soil and bryophyte/lichen ground layer). The analysis was performed with the adonis function in *Vegan* v.2.5.7 (Oksanen et al. 2019) using 1000 permutations. Pairwise comparisons between specific biocrust, cover type, and sites were conducted with the *Pairwise* package v.0.6.1 (Joerg-Henrik 2023), and *p*-values were adjusted using the Bonferroni correction. Lastly, we visualized beta diversity patterns using nonmetric multidimensional scaling (NMDS) based on GUniFrac distance matrices.

Comparison between bacterial community and soil physicochemical properties

The comparisons between soil physicochemical data and bacterial community composition from 16S rRNA and nifH genes sequencing was conducted integrating ASVs tables, sample data, and phylogenetic trees. Soil physicochemical data were processed using *phyloseq* and *dplyr* v.1.1.4 (Yarberry 2021). Normality of soil variables was assessed using the Shapiro–Wilk test; because some variables were normally distributed and others were not, we applied the nonparametric Kruskal–Wallis test (followed by Dunn's post hoc comparisons) to all datasets, which does not require data transformation. Additionally, we tested the multicollinearity in the soil physicochemical data from 16S rRNA and nifH genes, using the Spearman correlation analysis to reduce multicollinearity in the dataset, eliminating variables that were highly correlated ($r > 0.7$), and Variance Inflation Factor (VIF) for numerical variables (Akinwande et al. 2015). VIF values were used to identify redundant variables, with thresholds indicating no significant multicollinearity (VIF < 5), moderate multicollinearity ($5 \leq$ VIF < 10), and high multicollinearity (VIF $\geq$ 10). Removing variables with VIF $\geq$ 10 is a widely used strategy to mitigate multicollinearity in ecological datasets (Zuur et al. 2010; Akinwande et al. 2015). By eliminating only the most redundant predictors (K and Mg), we retained the bulk of meaningful soil parameters while preserving interpretability of downstream distance-based redundancy analysis (db-RDA) results.

To explore the relationships between soil physicochemical data and bacterial community composition, samples were converted into a microtable object using the *subset_samples*

and *phyloseq2meco* functions the *microeco* package v.1.10 (Liu et al. 2021). Differences in soil physicochemical properties between different biocrusts and cover types were analyzed using the Wilcoxon Rank Sum Test and ANOVA. Several soil parameters, including pH, EC, total nitrogen (N), total carbon (C), total sulfur (S), phosphorus (P), ammonium (NH_4), and organic matter percentage (perOM), were visualized through boxplots, which display the 25th and 75th percentiles as the lower and upper limits of the box, respectively, with the median represented as a central line. In addition, we performed a db-RDA to visualize the relationships between the soil physicochemical data and bacterial community composition. GUniFrac distances were used for db-RDA, and arrow projections were adjusted to highlight variable contributions. PERMANOVA was performed to test the significance of soil physicochemical properties, using the adonis3 function in the vegan package (Oksanen et al. 2019), 10 000 unrestricted permutations, and pairwise comparisons via *pairwise.adonis* with Bonferroni correction. Furthermore, the *envfit* function was used to assess the Pearson correlation between biocrusts, cover types, soil physicochemical properties, and bacterial community composition across different taxonomic levels (phylum, family, and genus). Adjustments for multiple comparisons were applied using the false discovery rate method, with separate adjustments performed for each soil physicochemical variable.

Exploring bacterial community functional profiles

We explored the functional profiles of bacterial community in the soil beneath different biocrusts and cover types from abandoned and rehabilitated mine. Functional profiles describe the predicted composition and relative abundance of metabolic functions within a microbial community (Douglas et al. 2020; Liu et al. 2021). We inferred the potential functional capabilities of bacterial communities using PICRUSt2 v.2.6.0 (Phylogenetic Investigation of Communities by Reconstruction of Unobserved States; Douglas et al. 2020). This tool predicts functions based on the phylogenetic composition of 16S rRNA gene sequences rather than the direct metagenomic or transcriptomic data. The previously generated ASV table was used to estimate functional contributions following the approach described by Douglas et al. (2020) and Liu et al. (2021).

Functional profiles of bacterial community in the soil beneath different biocrusts and cover types were assigned using the FAPROTAX database, which predicts ecological functions based on taxonomic identities, using databases derived from cultured microorganisms with known metabolic capabilities. This approach assumes that microorganisms with the same taxonomic identity share similar ecological functions, as observed in cultivated representatives. Both abundance-weighted and unweighted functional percentages were calculated (Liu et al. 2021). Functional groups, on the other hand, are sets of microorganisms that share similar metabolic or ecological functions, regardless of their phylogenetic relationship (e.g., nitrogen fixers, organic matter degraders, symbionts, or pathogens). These functional groups focus on the roles microorganisms play in specific ecological processes, independent of their taxonomic affiliation (Berg et al. 2020; Douglas et al. 2020; Liu et al. 2021).

To identify significant differences in functional potential across biocrusts and cover types, we applied a Wilcoxon test using the *cal_diff* function from the *microeco* package. The results were visualized with the *spe_func_perc* function to display the relative contribution of different bacterial functions. To assess the global relationships between functional profiles and bacterial community in the soil beneath different biocrusts and cover types of the *trans_env* function was used in the microeco object. Spearman correlations were computed to investigate specific relationships between functional profiles, bacterial community in the soil beneath different biocrusts and cover types, and physicochemical soil properties. The Spearman correlation analysis complemented the global insights provided by *trans_env*, offering a detailed understanding of the interactions. Heatmaps were generated using the *plot_cor* function. Transformation of data into long format for visualization, was performed using the *ggplot2* package (Wickham and Chang 2009).

Results

Bacterial composition

The filtered 16S rRNA gene of bacterial community in the soil beneath different biocrusts types (cyanobacteria, bryophytes, lichens), bare soil and bryophyte/lichen cover layer consisted of 103 samples (84 abandoned and 19 rehabilitated sites; Table S1). The bacterial community was represented by 2082 ASVs and mainly co-dominated by the phyla Acidobacteriota (23.53%), Proteobacteria (21.58%), Actinobacteriota (21.29%), and Chloroflexi (21.13%; Table S2).

The bacterial community in rehabilitated site was co-dominated by phyla Proteobacteria (6.94%), Acidobacteriota (6.49%), and Chloroflexi (5.44%). The most abundant families were Ktedonobacteraceae (6.49%) and Acidobacteriaceae (Subgroup 1; 5.31%). At the genus level, dominant taxa included *Afipia* (Proteobacteria; 4.01%), *Granulicella* (Acidobacteriota; 3.93%), and *Roseiarcus* (Proteobacteria; 2.59%; Fig. S1; Table S2). In the abandoned site, the bacterial community was co-dominated by Actinobacteriota (17.11%), Acidobacteriota (17.04%), and Chloroflexi (15.68%). The families more representative were Ktedonobacteraceae (14.42%) and Pseudonocardiaceae (12.21%). Dominant genera included *Prauserella* (Actinobacteriota; 19.88%), *Bryobacter* (Acidobacteriota; 9.68%), and *Afipia* (Proteobacteria: 9.46%; Fig. S1; Table S2). Furthermore, the bacterial composition also varied across biocrust and cover types and bare soil. In bare soil, the family Pseudonocardiaceae was most abundant (8.7%), with *Prauserella* (Actinobacteriota) as the dominant genus (14.2%). In cyanobacterial-dominated biocrusts, the family Xanthobacteraceae was most representative (1.9%), with *Prauserella* also being abundant (2.8%). In chlorolichens-dominated biocrusts, the family Acidobacteriaceae Subgroup 1 was dominant (4.0%), with *Bryobacter* as a key genus (4.7%). In moss-dominated biocrusts and the bryophyte/lichen cover layer, the family Ktedonobacteraceae was most abundant

Fig. 2. Bacterial diversity associated with biological soil crusts and cover types in the Preissac mine. Alpha diversity (Shannon, Simpson, and Faith's phylogenetic diversity index) of bacterial (16S rRNA gene) and diazotrophic (nifH gene) communities.

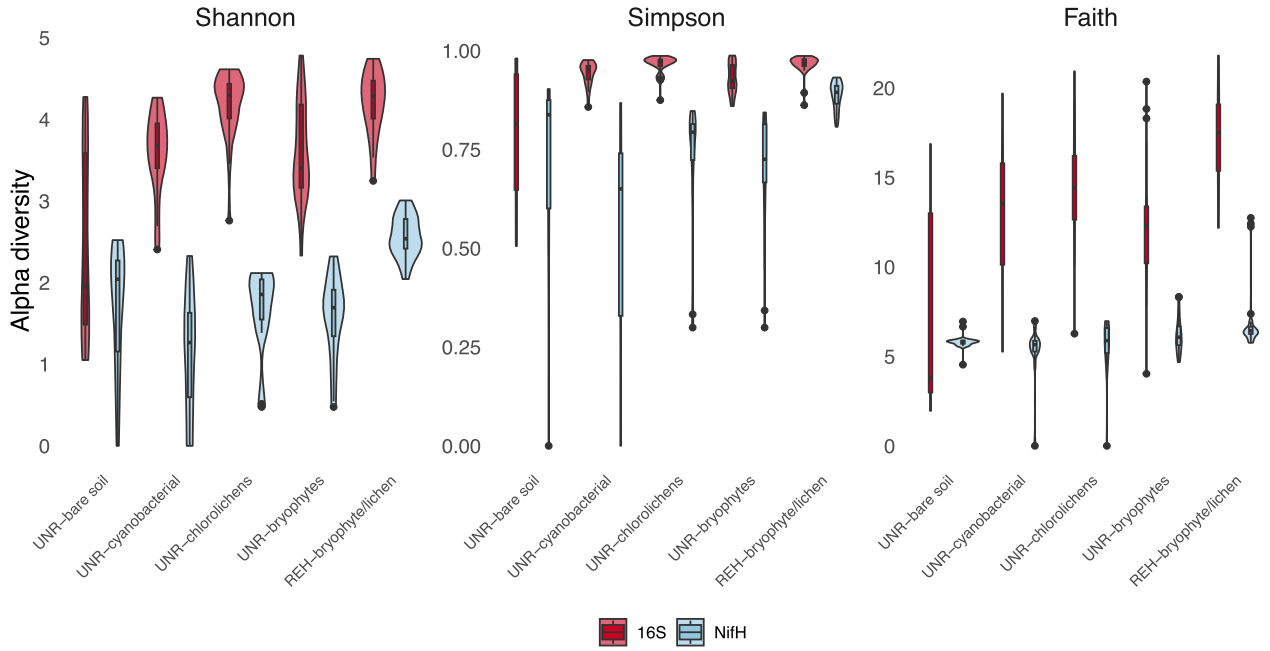

(9.9% and 6.9%, respectively). The genera *Afipia* (Proteobacteria, 4.0%) and *Granulicella* (Acidobacteriota, 3.9%) were particularly abundant in the bryophyte/lichen cover layer.

Amplicon data from the nifH locus resulted in 159 ASVs from 90 samples (65 from abandoned site and 25 from rehabilitated site; Table S1). The diazotrophic bacterial community was predominantly composed of the phyla Pseudomonadota (76.30%: rehabilitated 17.88%, abandoned 58.42%) and Cyanobacteria (23.52%: rehabilitated 13.16%, abandoned 10.36%), along with the family Comamonadaceae (68.82%). These same phyla and family were also dominant in the soil beneath all biocrusts and cover types (Fig. S2; Table S2). The genus *Variovorax* (Pseudomonadota) dominated the diazotrophic diversity for sites (56.91%: rehabilitated 12.44% and abandoned 44.47%) and biocrusts and cover types, with exception the cyanobacterial-dominated biocrusts where the genus *Hydrogenophaga* (Pseudomonadota; 2.4%) was more representative (Fig. S2; Table S2). Pairwise comparisons revealed significant differences in diversity between abandoned and rehabilitated mine sites, as well as biocrusts type and cover layers ($p < 0.01$) for both 16S rRNA gene data (Fig. S3) and nifH data (Fig. S4).

Bacterial diversity

Alpha diversity analysis revealed that both bacterial (16S rRNA gene) and diazotrophic (nifH) communities were more diverse in the rehabilitated site than in the abandoned site, regardless of the diversity index used (Figs. 2 and S5). When comparing biocrusts and cover types, in bacterial communities bare soil consistently exhibited the lowest diversity when compared to bryophyte/lichen cover layer (e.g., Shannon index: $Z = -5.37$, $p < 0.001$; Simpson index: $Z = -4.45$, $p < 0.001$) and cyanobacterial-dominated biocrusts (e.g., Shannon index: $Z = -2.02$, $p = 0.02$; Simpson index: $Z = -2.11$, $p = 0.01$; Fig. S6; Table S3). In diazotrophic (nifH) communities, post hoc test revealed significant differences in microbial diversity indices across biocrusts and cover types (Fig. S7). Bare soil had lower diversity compared to bryophyte/lichen cover layer (e.g., Shannon index: $Z = -3.77$, $p < 0.001$; Simpson index: $Z = -3.19$, $p = 0.001$; Table S3). On the other hand, we observed significant contrasts in bacterial and diazotrophic communities between bryophyte/lichen cover layer with bryophytes-dominated biocrusts (e.g., nifH gene, Shannon index: $Z = 5.49$, $p < 0.001$; Simpson index: $Z = 5.37$, $p < 0.001$) and cyanobacterial-dominated biocrusts (e.g., nifH gene, Shannon index: $Z = 6.26$, $p < 0.001$; Simpson index: $Z = 5.88$, $p < 0.001$) for all indexes (Fig. 2; Table S3).

We used NMDS to explore beta diversity in both bacteria (16S rRNA gene) and diazotrophic (nifH) communities (Figs. S7 and S8; R^2 values cited below derive from PERMANOVA on GUniFrac distances). For 16S rRNA gene, mining site differences explained 7% of community variation ($R^2 = 0.07$, $p = 0.001$), whereas biocrust and cover type differences explained 20% of community variation ($R^2 = 0.20$, $p < 0.001$). In contrast, the nifH gene showed a more balanced contribution, with mining sites explaining 11% ($R^2 = 0.11$, $p < 0.001$) and biocrust and cover type differences explaining 15% of community variation ($R^2 = 0.15$, $p < 0.001$; Table S4). Pairwise comparisons revealed significant diversity differences among multiple groups, with both markers consistently identifying cover types (bare soil and bryophyte/lichen cover layer) as distinct from other biocrust types (cyanobacterial-, chlorolichens-, and bryophytes-dominated biocrusts; Table S4).

Despite differences in richness (16S: 2082 ASVs and nifH: 159 ASVs), both datasets highlighted the influence

of biocrusts and cover types on the complexity of microbial beta-diversity in the underlying soil. Notably, the 16S data provided finer distinctions between cyanobacterial-dominated biocrusts and other biocrust and cover types, while the nifH marker showed only significant difference in cyanobacterial-dominated from bryophyte/lichen cover layer ($F = 6.38$, $R^2 = 0.141$, $p = 0.004$; p-adjusted = 0.04; Table S4).

Physicochemical soil properties

Analyses of soil physicochemical properties revealed significant variability across mine sites (χ^2 range = 0.01–20.5, $p < 0.001$ for 16S, and χ^2 range = 0.04–41.8, $p < 0.001$ for nifH, except for nitrogen and organic matter content $p > 0.01$), biocrust and cover types (χ^2 range = 41.8–62.7, $p < 0.001$ for 16S, and χ^2 range = 27.7–54.5, $p < 0.001$ for nifH; Figs. 3, 4, and S9; Table S5). For nitrogen (N), cyanobacterial-dominated biocrusts showed the highest nitrogen values, significantly different from bare soil, bryophyte/lichen cover, and all other biocrust types ($p < 0.001$ for 16S and nifH). EC and total carbon (C) exhibited significantly lower levels in bare soil compared to biocrust types and bryophyte/lichen cover layer ($p < 0.001$ for 16S and nifH). Sulfur (S) and phosphorus (P) levels were significantly higher in bryophytes-dominated biocrusts, and bryophyte/lichen cover layer compared to bare soil, chlorolichens- and cyanobacterial-dominated biocrusts ($p < 0.001$ for 16S and nifH). In contrast, pH and ammonium (NH_4) were significantly higher in bare soil and cyanobacterial-dominated biocrusts compared to chlorolichens-, bryophytes-dominated biocrusts, and bryophyte/lichen cover layer ($p < 0.001$ for 16S and nifH). Lastly, organic matter content (perOM) was significantly higher in chlorolichens-dominated biocrusts compared to other biocrust and cover types ($p < 0.001$ for 16S and nifH; Figs. 3 and S9; Table S5).

The VIF test revealed high multicollinearity among the soil physicochemical properties. As a result, potassium (VIF: 14.1 for 16S rRNA gene, 12.3 for nifH) and magnesium (VIF: 10.1 for 16S rRNA gene, 10 for nifH) were removed from the respective datasets (Table S5). The db-RDA model indicated a significant relationship between soil properties and microbial community taxonomic composition. For 16S, all variables, except N ($r^2 = 0.04$, $p = 0.12$), were key drivers, with the bacterial community exhibiting stronger relationships with EC ($r^2 = 0.18$, $p < 0.01$), pH ($r^2 = 0.37$, $p < 0.01$), S ($r^2 = 0.36$, $p < 0.01$), and P ($r^2 = 0.60$, $p < 0.01$; Fig. 4A; Table S5). Similarly, the diazotrophic community was significantly influenced by N ($r^2 = 0.19$, $p < 0.01$), C ($r^2 = 0.06$, $p < 0.01$), S ($r^2 = 0.19$, $p < 0.01$), P ($r^2 = 0.09$, $p < 0.01$), and NH_4 ($r^2 = 0.28$, $p < 0.01$; Fig. 4B; Table S5).

The bacterial community showed significant correlations with soil physicochemical properties. Positive Spearman's correlations were observed between Acidobacteriota and EC ($p = 0.28$, $p < 0.001$) and C ($p = 0.30$, $p < 0.05$); Actinobacteriota ($p = 0.41$, $p < 0.001$) and Firmicutes ($p = 0.33$, $p < 0.001$) with pH; Planctomycetota with C ($p = 0.28$, $p < 0.02$) and Chloroflexi with P ($p = 0.38$, $p < 0.001$). In contrast, negative correlations were found for Acidobacteriota, Proteobacteria, and Planctomycetota with pH ($p = -0.46$, $p < 0.001$; $p = -0.32$, $p < 0.003$; $p = -0.24$, $p < 0.03$, respectively), and for Actinobacteriota with EC and C ($p = -0.31$, $p < 0.01$; $p = -0.27$, $p < 0.02$). Additionally, Armatimonadota exhibited a negative correlation with NH_4 ($p = -0.39$, $p < 0.001$; Table S6). For the diazotrophic community, positive correlations were observed between Verrucomicrobiota and EC and NH_4 ($p = 0.37$, $p < 0.001$; $p = 0.35$, $p < 0.002$, respectively), as well as between Cyanobacteria with pH ($p = 0.33$, $p < 0.002$) and Bacillota with S ($p = 0.27$, $p < 0.04$). Conversely, Pseudomonadota showed a negative correlation with pH ($p = -0.33$, $p < 0.002$). In terms of bacterial communities' composition in the soil beneath different biocrusts and cover types. Bare soil exhibited positive correlations between Eremiobacterota, perOM, and EC ($p = 0.63$, $p < 0.02$; $p = 0.65$, $p < 0.03$, respectively). Cyanobacterial-dominated biocrusts showed a positive correlation with the phylum Cyanobacteria and C ($p = 0.72$, $p < 0.04$). In bryophyte/lichen cover layer, Actinobacteriota and Myxococcota displayed positive correlations with perOM ($p = 0.73$, $p < 0.01$; $p = 0.64$, $p < 0.04$), while Proteobacteria showed negative correlations with C and EC ($p = -0.76$, $p < 0.001$; $p = -0.68$, $p < 0.03$; Table S6).

On the other hand, we identified over 40 (bacterial community) and 13 (diazotrophic organisms) significant correlations at the family level, primarily associated with pH, and more than 60 (bacterial community) and 10 (diazotrophic organisms) correlations at the genus level (Table S6). The bacterial community showed positive associations between families and cyanobacterial-dominated biocrust with EC, N, and C ($p = 0.80$, $p < 0.03$; $p = 0.80$, $p < 0.02$; $p = 0.80$, $p < 0.04$, respectively), whereas bryophyte/lichen cover layer correlated negatively with EC and N ($p = -0.85$, $p < 0.001$; $p = -0.86$, $p < 0.001$). Among the genera associated with cyanobacterial-dominated biocrust with EC ($p = -0.80$, $p < 0.01$), chlorolichens-dominated biocrust with S ($p = 0.70$, $p < 0.02$), and bryophytes-dominated biocrust with N, C, EC, and NH_4 ($p = 0.84$, $p < 0.001$; $p = 0.83$, $p < 0.001$; $p = 0.69$, $p < 0.02$; $p = 0.75$, $p < 0.03$, respectively), while bryophyte/lichen cover layer again showed inverse patterns with EC/N (Table S6). Notably, diazotrophic organisms in bare soil correlated positively between S with Comamonadaceae ($p = 0.86$, $p < 0.001$) and Geminicoccaceae ($p = 0.77$, $p < 0.03$); whereas Tolypothrichaceae with pH ($p = 0.84$, $p < 0.01$), and bryophytes-dominated biocrust with S ($p = 0.63$, $p < 0.03$; Table S6).

Functional profiles in bacterial community

Analyses of bacterial functional profiles revealed distinct metabolic specialization under different biocrusts and cover types (Table S7). Communities showed strong functional associations with energy production and nitrogen/carbon cycling, but weaker links to iron cycling, cyanobacterial metabolism, and host–microbe interactions (Fig. 5A; Table S7).

Spearman correlation analyses revealed distinct functional adaptations in the rehabilitated site's bacterial community. Positive correlations emerged between photoautotrophic processes (including sulfur-oxidizing types) and soil properties like sulfur (S; $p = 0.71$, $p < 0.01$) and organic matter content (perOM; $p = 0.62$, $p < 0.03$). In contrast, significant

Fig. 3. Soil physicochemical properties of the bacterial (16S rRNA gene) community under different biocrusts and cover types in the Preissac mine. Boxes limit the 25th and 75th percentiles with the median shown as a line. Error bars present the 1st and 99th percentiles. Significant differences among groups ($p < 0.05$) are indicated by different letters; groups sharing the same letter are not significantly different.

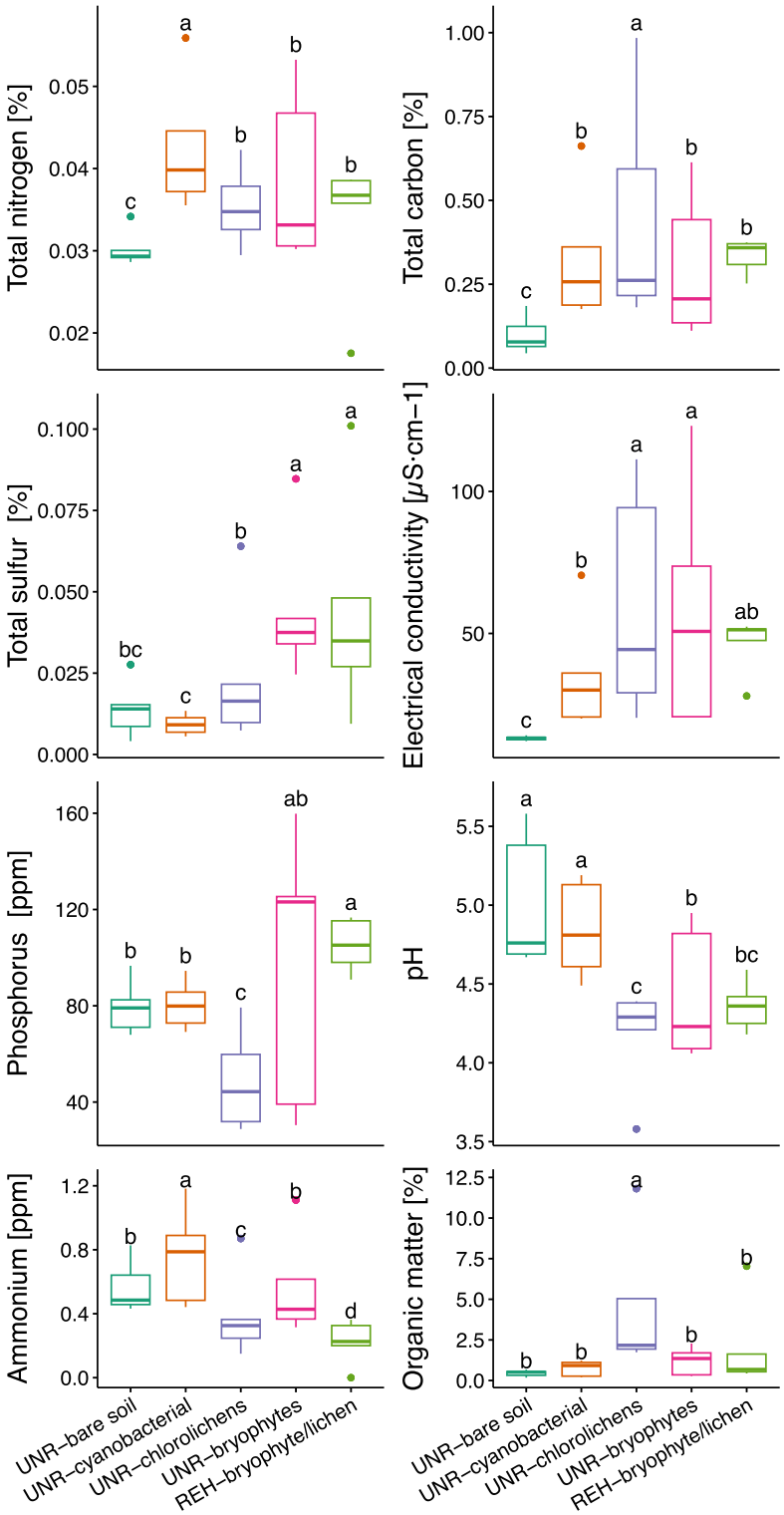

negative correlations were found between aerobic chemoheterotrophy ($p = -0.62$, $p < 0.03$) and chemoheterotrophy ($p = -0.63$, $p < 0.03$) with carbon content (Fig. 5B; Table S7). Furthermore, in the abandoned site, bacterial community functional profiles were primarily linked to chemoheterotrophic and photoheterotrophy associations with EC

Fig. 4. Bacterial community composition in the soil beneath different biocrusts and cover types, shown as a distance-based redundancy analysis (db-RDA) ordination based on GUniFrac distances. Arrows represent soil physicochemical variables significantly correlated with community composition ($p < 0.05$). (A) Based on amplicon 16S data. (B) Based on amplicon nifH data. Colors indicate sites and symbols indicate biocrust and cover types. perOM, percent organic matter; EC, electrical conductivity.

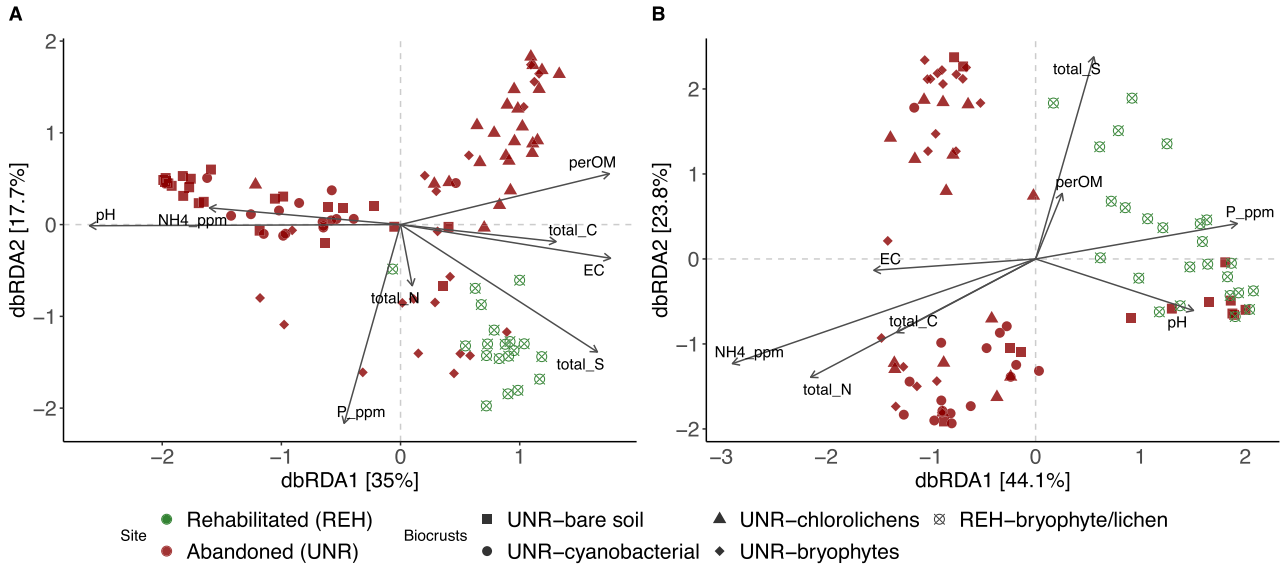

($p = 0.32$, $p < 0.02$; $p = 0.41$, $p < 0.001$), C ($p = 0.36$, $p < 0.01$; $p = 0.44$; $p < 0.001$;), perOM ($p = 0.44$, $p < 0.001$), while correlating negatively with associations with NH_4 ($p = -0.31$, $p < 0.03$), P ($p = -0.37$, $p < 0.001$; $p = -0.35$, $p < 0.01$), and pH ($p = -0.52$, $p < 0.001$; $p = -0.33$, $p < 0.03$) and processes showing particularly strong correlations (Fig. 5B; Table S7).

Additionally, the functional profiles associated with anoxygenic photoautotrophy and sulfur content exhibited positive correlations with bryophyte/lichen cover layer ($p = 0.78$, $p < 0.02$), indicating sulfur oxidation can as a key functional pathway in these environments. On the other hand, significant negative correlations between chemoheterotrophy, aerobic chemoheterotrophy with pH ($p = -0.78$, $p < 0.02$; $p = -0.77$, $p < 0.01$) and phototrophy, with P ($p = -0.73$, $p < 0.03$) in bryophytes-dominated biocrusts, suggesting reduced heterotrophic activity under acidic and saline conditions (Fig. 5C; Table S7).

Host–microbe interactions (including pathogenic and symbiotic relationships) emerged as the second major functional group in the Preissac mine ecosystems. This group showed a significant correlation with intracellular parasites ($p = -0.77$, $p < 0.001$, exclusive to the rehabilitated site), human pathogens, human-associated microbes, and animal parasites or symbionts ($p < 0.05$). Distinct environmental drivers were observed between sites: rehabilitated areas showed negative associations with EC, P, and S, while abandoned sites exhibited positive correlations with EC, perOM, and C alongside negative pH relationships (Fig. 5B; Table S7). Furthermore, the bacterial community related with carbon cycle group exhibited functional profiles correlated to cellulolysis ($p < 0.01$), with a significant relationship between perOM ($p < 0.001$), and C ($p < 0.001$) at both mine sites. The abandoned site and the bryophytes-dominated biocrusts showed a significant negative correlation with pH ($p = -0.56$, $p < 0.001$).

Likewise, the nitrogen cycle group displayed significant relationships between functional profiles associated with nitrifying functions and S ($p < 0.01$). Additionally, a significant negative correlation was observed between nitrogen fixation and perOM ($r = -0.62$, $p < 0.03$), ureolysis and EC ($r = -0.61$, $p < 0.03$), and S ($r = -0.70$, $p < 0.01$) in the rehabilitated site. In contrast, the abandoned site showed significant relationships only with ureolysis, which exhibited a positive correlation with EC ($p = 0.33$, $p < 0.01$), perOM ($p = 0.34$, $p < 0.01$), and C ($p = 0.35$, $p < 0.01$), as well as a negative correlation with pH ($p = -0.48$, $p < 0.001$). At the biocrust level, some correlations were observed, but they were not statistically significant (Fig. 5C). Also, the Iron cycle group demonstrated processes related to iron respiration, with a significant positive relationship between perOM ($p = 0.49$, $p < 0.001$), EC ($p = 0.43$, $p < 0.001$), and C ($p = 0.37$, $p < 0.001$) in the abandoned site, and NH_4 ($p = 0.64$, $p < 0.02$) in the rehabilitated site. Besides, a significant negative correlation was found between pH ($p = -0.44$, $p < 0.001$) and P ($p = -0.36$, $p < 0.01$) in the abandoned site. Finally, cyanobacteria metabolism and photosynthesis group showed a significant correlation with nonphotosynthetic cyanobacteria functional profile ($p < 0.001$). In the rehabilitated site, the bacterial community exhibited positive correlations with N, whereas in the abandoned site it showed negative correlations with P and pH (Fig. 5B; Table S7).

Discussion

This study characterizes bacterial composition and functional profiles in soils under biocrusts during ecological succession at abandoned mine sites in Western Boreal Quebec, Canada's forest. Key findings include: (1) physicochemical properties (e.g., pH, EC, S) were related to bacterial diversity (db-RDA, $R^2 = 0.20$), with Proteobacteria dominating re-

Fig. 5. Functional profiles and physicochemical soil properties of bacterial (16S rRNA gene) community under biocrusts and cover types in Preissac mine. (A) Relative abundance. (B and C) Heatmap based on a Spearman correlation. (B) Preissac mine (rehabilitated and abandoned sites). (C) Biocrusts and cover types. Red and blue colors indicate positive and negative correlations between the variables, respectively. Significant differences ($p < 0.05$) are marked by asterisks.

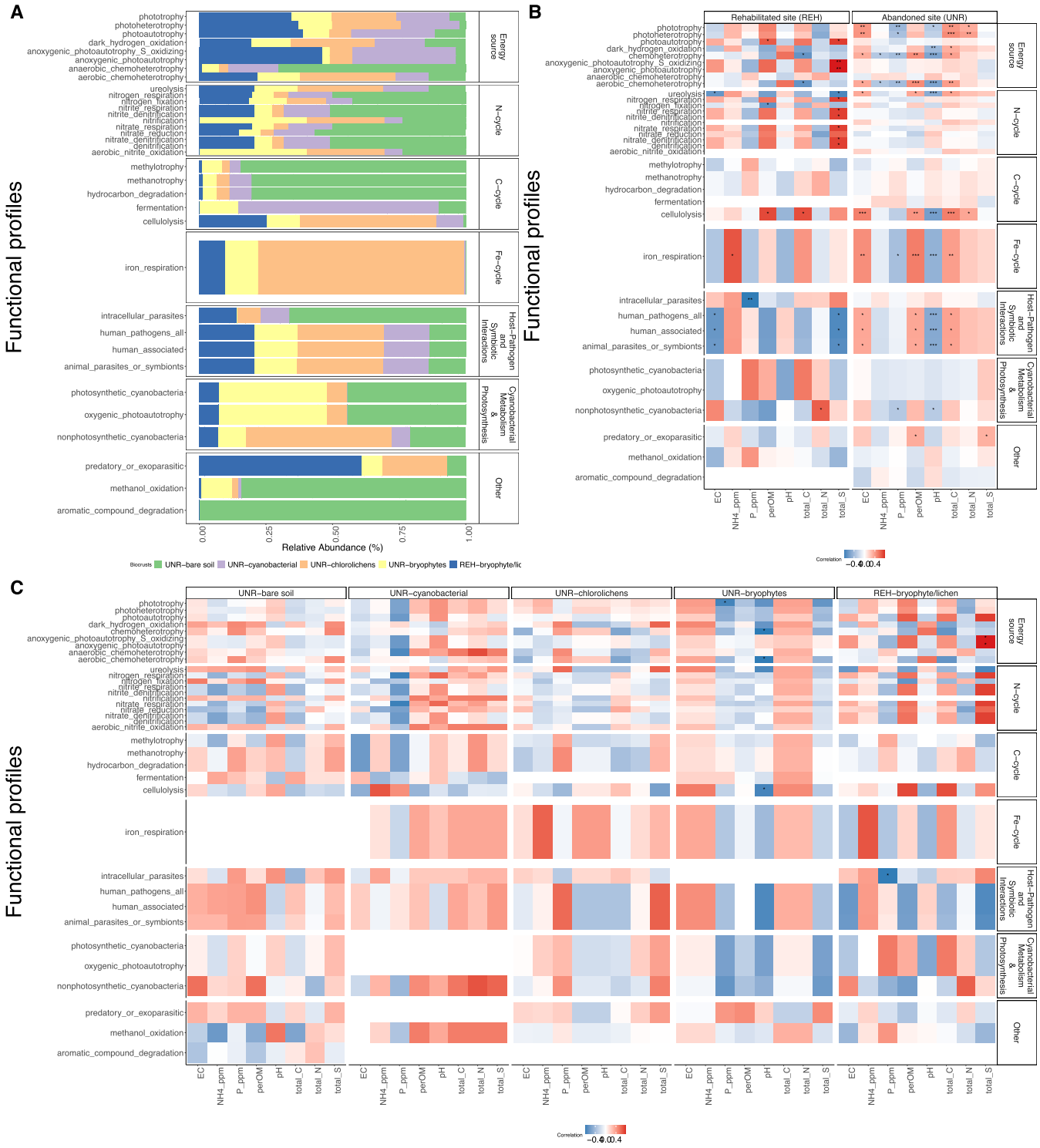

habilitated sites (6.9%)—indicating nutrient-rich conditions—versus Actinobacteriota (17.1%) in abandoned sites, consistent with oligotrophic adaptation; (2) functional transitions from chemoheterotrophy to photoautotrophy/nitrification in late succession were linked to sulfur oxidation dynamics (Spearman's $\rho = 0.6$, $p < 0.05$), with anoxygenic photoautotrophs driving S-oxidation in bryophyte/lichen cover layer (Fig. 5; Table S7). These results support both hypotheses: soil properties and bacterial communities are associated, and succession enhances diversity/functionality, highlighting

bacterial community under biocrusts as ecosystem engineers in mine rehabilitation. This process is particularly relevant in mine tailings, where instability and nutrient scarcity hinder plant establishment (Harris 2009; Guittonny and Bussière 2020; Watson et al. 2022; Geng et al. 2023).

Biocrusts and microbial composition

Biocrusts play a critical role in ecosystem restoration, particularly in post-mining environments (Harris 2009; Li et al. 2024). The composition of the bacterial community in the Preissac mine varies not only between the rehabilitated and abandoned sites but also depending on the type of biocrust and cover present. Despite these differences, the bacterial community was dominated by Acidobacteriota, Proteobacteria, and Actinobacteriota, while the diazotrophic community was primarily composed of Pseudomonadota and Cyanobacteria. This composition is consistent with previous studies on microbial communities in biocrust present in desert environments across several continents (Zhang et al. 2016; Maier et al. 2018; Moreira-Grez et al. 2019), mesic forests (Glaser et al. 2022), and the subarctic region of North America with mosses (Holland-Moritz et al. 2018, 2021; Stuart et al. 2021; Renaudin et al. 2022; Escolástico-Ortiz et al. 2023).

Beyond these broad taxonomic patterns, specific genera within biocrusts reveal important ecological functions that may influence succession. For instance, based on relative abundance profiles, the presence of *Bryobacter*, an aerobic chemo-organotroph, in biocrusts dominated by bryophytes and lichens aligns with its role as a heterotrophic degrader in organic matter-rich environments (Alcaraz et al. 2018). *Bryobacter* plays a key role in carbon cycling and may contribute to bryophyte nutrition (Kulichevskaya et al. 2010; Escolástico-Ortiz et al. 2023). Similarly, *Variovorax* showed a progressive increase in relative abundance, transitioning from bare soil to bryophytes-dominated biocrusts. *Variovorax*, known for its broad-spectrum metabolic capabilities, modulates plant hormone levels by degrading auxins, thereby preventing root growth inhibition and supporting root development (Sánchez-Cañizares et al. 2017; Finkel et al. 2020). Furthermore, *Variovorax* plays a key role in plant growth and environmental adaptability, particularly in the nitrogen cycle under stress conditions (Flores-Duarte et al. 2022; Ghimire et al. 2022; Acuña et al. 2024). Both *Bryobacter* and *Variovorax* contribute to shifts in the soil bacterial community, suggesting a potential role in biocrust dynamics and ecological succession (Xue et al. 2017; Sui et al. 2022).

Soil physicochemical properties and biocrust development

Our study demonstrates that bacterial community under biocrusts and soil geochemistry are correlated, with distinct differences in soil properties across biocrust types. Bare soil exhibited lower EC and carbon (C) levels compared to all biocrust types in Preissac mine, underscoring the role of biocrusts in carbon accumulation and nutrient stabilization (Maier et al. 2018; McLeod et al. 2021; Weber et al. 2022; Witzgall et al. 2024). In addition, biocrusts can contribute to approximately 7% carbon fixation and 40%–70% nitrogen fixation in drylands and the global terrestrial ecosystems, reinforcing their essential function in ecosystem recovery (Elbert et al. 2012; Karsten et al. 2014; Weber et al. 2015; Rodriguez-Caballero et al. 2018). The increased organic matter observed in chlorolichens-dominated biocrusts further supports the role of these communities in carbon sequestration and soil enrichment (Liao et al. 2024; Wu et al. 2022). Additionally, the observed differences in nitrogen (N) and phosphorus (P) content among biocrust and cover types highlight their role in biogeochemical cycling. Notably, cyanobacterial-dominated biocrusts exhibited the highest nitrogen levels, in contrast to bare soil and other biocrust types, likely due to their well-documented nitrogen-fixing capabilities (Deng et al. 2020; Cowden et al. 2022; Renaudin et al. 2022). These patterns suggest that, during primary succession, nitrogen accumulates or redistributes as biocrusts mature, driven by changes in microbial communities and ecosystem functions—as observed in some mines, boreal forests, and deserts (Deng et al. 2020; Cowden et al. 2022; Renaudin et al. 2022).

In contrast, bryophytes-dominated biocrusts and bryophyte/lichen cover layer showed higher sulfur (S) and phosphorus (P) levels, supporting previous findings that biocrusts enhance phosphorus transformation and retention in nutrient-limited environments (Wu et al. 2022; Li et al. 2024; Liao et al. 2024). The interplay between N, P, and S cycling within these biocrusts may contribute to long-term soil fertility and microbial diversity, key factors in ecosystem restoration (Renaudin et al. 2022; Geng et al. 2023; Liao et al. 2024; Sun et al. 2024). Finally, soil pH and ammonium (NH_4) concentrations were higher in bare soil and cyanobacterial-dominated biocrusts compared to later successional biocrusts. This pattern aligns with previous studies suggesting that cyanobacterial activity can initially increase soil pH before later-stage biocrusts, particularly in mine tailings and boreal forest where bryophytes and lichens, modulate pH to favor more complex microbial interactions (Nyenda et al. 2019; Renaudin et al. 2022; Liao et al. 2024; Sun et al. 2024).

Influence of soil physicochemical properties on microbial functionality

The role of biocrusts in ecosystem succession is highlighted by their strong influence on microbial functional profiles and soil physicochemical properties (Duan et al. 2024; Zhang 2024). At both rehabilitated and abandoned Preissac mine sites, the bacterial communities beneath these biocrusts regulate key biogeochemical cycles—including carbon, nitrogen, sulfur, and iron—by hosting microbes with diverse metabolic capabilities. Previous studies have demonstrated that these microbial assemblages are essential for biocrusts formation and the reclamation of mining tailings (Langille et al. 2013; Sun et al. 2024). This regulatory function is suggested by the associations observed between microbial functional groups and soil parameters, particularly within the energy, carbon, nitrogen, and iron cycles. For example, carbon and nitrogen fixation may contribute to enhancing soil fertility and stability (Nyenda et al. 2019; Liao et al. 2024). Additionally, these communities appear to be involved in sul-

fur and iron cycling, processes that are vital for maintaining soil health and supporting plant growth (Trivedi et al. 2020; Sun et al. 2024). Collectively, these functions underscore the importance of bacterial communities under biocrusts in regulating nutrient availability and promoting ecological restoration in degraded environments.

For instance, in the rehabilitated site, bryophyte/lichen cover layer exhibited positive relationships between anoxygenic photoautotrophy and sulfur content, which may indicate that sulfur oxidation could represent an important functional pathway in these environments (Kushkevych et al. 2024; Sun et al. 2024). Similarly, bryophytes-dominated biocrusts were less associated with chemoheterotrophy and phototrophy under acidic and saline conditions, which could indicate a potential decrease in heterotrophic activity, perhaps linked to slower organic matter decomposition. This pattern was confirmed by significant negative correlations between pH and heterotrophic functional groups. These findings align with previous research on microbial communities in intertidal estuarine soils, where microbial functional profiles are closely linked to environmental gradients such as salinity and organic matter content (Flores-Duarte et al. 2022; Zhang et al. 2023; Wu et al. 2024). Moreover, studies on alpine and temperate grasslands of China have shown that soil microbial community structures are influenced by local biogeochemical conditions, reinforcing the observed relationships between microbial functional potential and soil properties in this study (Oh et al. 2016; Duan et al. 2024). Furthermore, nitrogen metabolism and oxidative phosphorylation may play a crucial role in regulating nitrogen and phosphorus cycling, essential for pollution control strategies (Li et al. 2024; Liao et al. 2024).

In addition to their role in primary productivity, biocrusts may be involved in host-pathogen and symbiotic interactions, particularly in the rehabilitated site, where correlations were found with intracellular parasites and human-associated microbes. These relationships were negative with phosphorus, EC, and sulfur, suggesting a potential link between nutrient availability and microbial interactions. This could be consistent with microbial communities that exhibit functional plasticity in response to environmental perturbations, including nutrient enrichment and pollution (Oh et al. 2016; Zhang et al. 2023). Similarly, cyanobacterial metabolism and photosynthesis group showed a notable relationship with nitrogen availability, further supporting the role of bacterial communities and biocrusts in facilitating nitrogen cycling in degraded environments (Eldridge and Greene 1994; Deng et al. 2020; Chowaniec et al. 2024). This was evidenced by the positive linkages between nitrogen and cyanobacterial metabolism in the rehabilitated site. The presence of nitrogen fixation processes in Preissac mine also reflects patterns observed in other environments, where nitrogen-related functional profiles are shaped by variations in soil properties (Elbert et al. 2012; Oh et al. 2016; Chowaniec et al. 2024; Duan et al. 2024).

Finally, the associations found between ureolysis and soil organic matter in the abandoned site, and the observed relationships between carbohydrate and amino acid metabolism, may suggest a potential capacity for pollutant degradation, as previously noted in microbial communities within drinking water systems (Chen et al. 2021; Li et al. 2024). This is further supported by the adaptability of microbial communities in response to land abandonment, where shifts in microbial functional profiles, such as methanotrophic bacteria, could indicate an ecological strategy to cope with declining nutrient levels (Wu et al. 2024). For example, the association of these bacteria with peat may increase the source of carbon in plants and help regulate methane emissions into the atmosphere (Kostka et al. 2016). These results underscore the importance of bacterial community under biocrusts as ecological engineers that mediate microbial functional diversity and ecosystem recovery through their influence on soil chemistry and microbial interactions.

Conclusion

Our study provides evidence that bacterial communities beneath biocrusts markedly enhance soil stabilization, nutrient cycling, and microbial interactions at both abandoned and rehabilitated mine sites in Western Boreal Quebec forest, (Cowden et al. 2022; Duan et al. 2024). Shifts in bacterial composition, diversity, and predicted functionality across successional stages were associated with variation in soil properties, highlighting their potential as bioindicators of ecosystem recovery. Cyanobacterial-dominated biocrusts were associated with nitrogen fixation and organic matter accumulation, while bryophytes/lichen cover layer drive phosphorus and sulfur dynamics, supporting the model of biocrust succession in mine tailings from cyanobacteria to more complex communities dominated by lichens and bryophytes (Lan et al. 2013; Maier et al. 2018; Chowaniec et al. 2024). Later-stage biocrusts, dominated by lichens and bryophytes, exhibit higher nitrogen fixation rates and greater photosynthetic efficiency, (Su et al. 2011; Barger et al. 2016; Salazar et al. 2022; Chowaniec et al. 2024), potentially enhancing nutrient cycling. These mature biocrusts can improve soil fertility but also increase the bioavailability of essential nutrients such as nitrogen and phosphorus, which are typically scarce in mine tailings (Sun et al. 2024). Given the central role of bacterial communities under biocrusts in driving ecological succession at abandoned mining sites in Western Boreal Quebec forest, our findings underscore the importance of develop strategies for propagating, facilitating, and reintroducing biocrusts to restore mine tailings and fully harness their ecological services.

Acknowledgements

GFBP thanks LFMT and AS for their support and assistance throughout the work.

Article information

History dates

Received: 1 May 2025
Revised: 18 December 2025
Accepted: 5 January 2026

Accepted manuscript online: 16 January 2026
Version of record online: 23 February 2026

Data availability
Raw sequence data were deposited in the NCBI Sequence Read Archive (SRA) under the bioproject number PRJNA1225235 with their respective accession numbers. The datasets, metadata, and scripts generated and/or analysed during the current study are openly available in the Github repository: https://github.com/gpenalozabojaca/Biocrusts-on-post-mining.git.

Author information

Author ORCIDs
Gabriel F. Peñaloza-Bojacá https://orcid.org/0000-0001-7085-9521
Laura Hjartarson https://orcid.org/0009-0003-5067-2665
Marta Alonso-Garcia https://orcid.org/0000-0002-2935-7754
Juan Carlos Villarreal Aguilar https://orcid.org/0000-0002-0770-1446
Line Rochefort https://orcid.org/0000-0001-8450-0376
Mélina Guêné-Nanchen https://orcid.org/0000-0002-7737-8840

Author notes
Gabriel F. Peñaloza-Bojacá and Laura Hjartarson contributed equally to this work.

Author contributions
Conceptualization: GFP, LH, MA, JCVA, LR, MG
Data curation: GFP, LH, MA
Formal analysis: GFP, LH
Funding acquisition: JCVA, MG
Investigation: GFP, LH, MA, JCVA, LR, MG
Methodology: GFP, LH, MA, JCVA, LR
Project administration: JCVA, LR, MG
Resources: MA
Supervision: MA, JCVA, LR, MG
Validation: GFP, JCVA, LR, MG
Visualization: GFP, MA, JCVA
Writing – original draft: GFP, LH, MA, JCVA, LR, MG
Writing – review & editing: GFP, LH, MA, JCVA, LR, MG

Competing interests
The authors declare no conflict of interest.

Funding information
This work was funded and supported by Fonds de recherche du Québec—Nature et technologies (FRQNT) through the Programme de recherche en partenariat sur le développement durable du secteur minier-II (2020-MN-285996) and a postdoctoral fellowship (https://doi.org/10.69777/352787).

Supplementary material
Supplementary data are available with the article at https://doi.org/10.1139/cjm-2025-0090.

References
Acuña, J.J., Rilling, J.I., Inostroza, N.G., Zhang, Q., Wick, L.Y., Sessitsch, A., and Jorquera, M.A. 2024. Variovorax sp. strain P1R9 applied individually or as part of bacterial consortia enhances wheat germination under salt stress conditions. Sci. Rep. **14**: 2070. doi:10.1038/s41598-024-52535-0.

Akinwande, M.O., Dikko, H.G., and Samson, A. 2015. Variance Inflation Factor: as a condition for the inclusion of suppressor variable(s) in regression analysis. Open J. Stat. **05**: 754–767. doi:10.4236/ojs.2015.57075.

Alcaraz, L.D., Peimbert, M., Barajas, H.R., Dorantes-Acosta, A.E., Bowman, J.L., and Arteaga-Vázquez, M.A. 2018. Marchantia liverworts as a proxy to plants' basal microbiomes. Sci. Rep. **8**: 12712. doi:10.1038/s41598-018-31168-0.

Bell-Doyon, P., Bellavance, V., Bélanger, L., Mazerolle, M.J., and Villarreal, A.J.C. 2022. Bacterial, fungal, and mycorrhizal communities in the soil differ between clearcuts and insect outbreaks in the boreal forest 50 years after disturbance. For. Ecol. Manage. **523**: 120493. doi:10.1016/j.foreco.2022.120493.

Bell-Doyon, P., Laroche, J., Saltonstall, K., and Villarreal, J.C. 2020. Specialized bacteriome uncovered in the coralloid roots of the epiphytic gymnosperm, Zamia pseudoparasitica. Environ. DNA, 1–11. doi:10.1002/edn3.66.

Belnap, J., Weber, B., and Büdel, B. 2016. Biological soil crusts as an organizing principle in drylands. In Biological soil crusts: an organizing principle in drylands. Ecological studies. Vol. 226. Springer International Publishing, Cham. doi:10.1007/978-3-319-30214-0_1.

Berg, G., Rybakova, D., Fischer, D., Cernava, T., Vergès, M.-C.C., Charles, T., et al. 2020. Correction to: Microbiome definition re-visited: old concepts and new challenges. Microbiome, **8**: 119. doi:10.1186/s40168-020-00905-x.

Boily, M. 1995. Pétrogenèse du batholite de Preissac—Lacorne: implications pour la métallogénie des gisements de métaux rares. Et 93-05. Direction générale de l'exploration géologique et minérale. Québec, Canada.

Bray, R.H., and Kurtz, L.T. 1945. Determination of total, organic, and available forms of phosphorus in soils. Soil Sci. **59**: 39–46. doi:10.1097/00010694-194501000-00006.

Callahan, B., McMurdie, P., Rosen, M., Han, A., Johnson, A., and Holmes, S. 2016. DADA2: high-resolution sample inference from Illumina amplicon data. Nat. Methods, **13**: 581–583. doi:10.1038/nmeth.3869.

Callahan, B., McMurdie, P.J., and Holmes, S.P. 2017. Exact sequence variants should replace operational taxonomic units in marker-gene data analysis. ISME J. **11**: 2639–2643. doi:10.1038/ismej.2017.119.

CANMET. 1976. Certified and provisional reference materials available from the Canada centre for mineral and energy technology as of 1976. Supply and Services Canada, Ottawa, Canada.

CEAEQ. 2014. Détermination des métaux et du phosphore assimilables : méthode par spectrométrie de masse à source ionisante au plasma d'argon, MA. 200 – Mét-P ass. 1.0. Ministère du Développement durable, l'Environnement la Lutte contre les Chang. Clim. du Québec, **11**: 15.

Chamizo, S., Cantón, Y., Miralles, I., and Domingo, F. 2012. Biological soil crust development affects physicochemical characteristics of soil surface in semiarid ecosystems. Soil Biol. Biochem. **49**: 96–105. doi:10.1016/j.soilbio.2012.02.017.

Chen, J., Bittinger, K., Charlson, E.S., Hoffmann, C., Lewis, J., Wu, G.D., et al. 2012. Associating microbiome composition with environmental covariates using generalized UniFrac distances. Bioinformatics, **28**: 2106–2113. doi:10.1093/bioinformatics/bts342.

Chen, L., Zhai, Y., van der Mark, E., Liu, G., van der Meer, W., and Medema, G. 2021. Microbial community assembly and metabolic function in top layers of slow sand filters for drinking water production. J. Clean. Prod. **294**: 126342. doi:10.1016/j.jclepro.2021.126342.

Chowaniec, K., Styburski, J., Kozioł, S., Pisańska, Z., and Skubała, K. 2024. Dune blowouts as microbial hotspots and the changes of over-

all microbial activity and photosynthetic biomass along with succession of biological soil crusts. Microb. Ecol. **87**: 22. doi:10.1007/s00248-023-02333-4.

CIM. 2023. Mines & Environment 2025 [WWW Document]. Canadian Institute of Mining, Metallurgy and Petroleum. Available from https://mines-et-environnement.cim.org/visites-des-site/ [accessed 3 February 2025].

Cowden, P., Hanner, R., Collis, B., Kuzmina, M., Conway, A., Ivanova, N., and Stewart, K. 2022. Early successional changes in biological soil crust community assembly and nutrient capture in mining impacted landscapes. Soil Biol. Biochem. **175**: 108841. doi:10.1016/j.soilbio.2022.108841.

Davis, N.M., Proctor, D.M., Holmes, S.P., Relman, D.A., and Callahan, B.J. 2018. Simple statistical identification and removal of contaminant sequences in marker-gene and metagenomics data. Microbiome, **6**: 226. doi:10.1186/s40168-018-0605-2.

DeLuca, T., Zackrisson, O., Nilsson, M., and Sellstedt, A. 2002. Quantifying nitrogen-fixation in feather moss carpets of boreal forests. Nature, **419**: 917–920. doi:10.1038/nature01051.

Deng, S., Zhang, D., Wang, G., Zhou, X., Ye, C., Fu, T., et al. 2020. Biological soil crust succession in deserts through a 59-year-long case study in China: how induced biological soil crust strategy accelerates desertification reversal from decades to years. Soil Biol. Biochem. **141**: 107665. doi:10.1016/j.soilbio.2019.107665.

Dou, W., Xiao, B., Revillini, D., and Delgado-Baquerizo, M. 2024. Biocrusts enhance soil organic carbon stability and regulate the fate of new-input carbon in semiarid desert ecosystems. Sci. Total Environ. **918**: 170794. doi:10.1016/j.scitotenv.2024.170794.

Douglas, G.M., Maffei, V.J., Zaneveld, J.R., Yurgel, S.N., Brown, J.R., Taylor, C.M., et al. 2020. PICRUSt2 for prediction of metagenome functions. Nat. Biotechnol. **38**: 685–688. doi:10.1038/s41587-020-0548-6.

Duan, Y., Li, Y., Zhao, J., Zhang, J., Luo, C., Jia, R., and Liu, X. 2024. Changes in microbial composition during the succession of biological soil crusts in Alpine Hulun Buir Sandy Land, China. Microb. Ecol. **87**: 43. doi:10.1007/s00248-024-02359-2.

Elbert, W., Weber, B., Burrows, S., Steinkamp, J., Büdel, B., Andreae, M.O., and Pöschl, U. 2012. Contribution of cryptogamic covers to the global cycles of carbon and nitrogen. Nat. Geosci. **5**: 459–462. doi:10.1038/ngeo1486.

Eldridge, D., and Greene, R. 1994. Microbiotic soil crusts—a review of their roles in soil and ecological processes in the rangelands of Australia. Aust. J. Soil Res. **32**: 389. doi:10.1071/SR9940389.

Eldridge, D.J., Reed, S., Travers, S.K., Bowker, M.A., Maestre, F.T., Ding, J., et al. 2020. The pervasive and multifaceted influence of biocrusts on water in the world's drylands. Global Change Biol. **26**: 6003–6014. doi:10.1111/gcb.15232.

Escolástico-Ortiz, D.A., Blasi, C., Bellenger, J.-P., Derome, N., and Villarreal-A, J.C. 2023. Differentially abundant bacteria drive the N2-fixation of a widespread moss in the forest-tundra transition zone. Symbiosis, **90**: 193–211. doi:10.1007/s13199-023-00930-y.

Faith, D.P. 1992. Conservation evaluation and phylogenetic diversity. Biol. Conserv. **61**: 1–10. doi:10.1016/0006-3207(92)91201-3.

Finkel, O.M., Salas-González, I., Castrillo, G., Conway, J.M., Law, T.F., Teixeira, P.J.P.L., et al. 2020. A single bacterial genus maintains root growth in a complex microbiome. Nature, **587**: 103–108. doi:10.1038/s41586-020-2778-7.

Flores-Duarte, N.J., Pérez-Pérez, J., Navarro-Torre, S., Mateos-Naranjo, E., Redondo-Gómez, S., Pajuelo, E., and Rodríguez-Llorente, I.D. 2022. Improved Medicago sativa Nodulation under Stress Assisted by Variovorax sp. Endophytes. Plants, **11**: 1091. doi:10.3390/plants11081091.

Gadd, G.M. 2010. Metals, minerals and microbes: geomicrobiology and bioremediation. Microbiology, **156**: 609–643. doi:10.1099/mic.0.037143-0.

Gao, L., Bowker, M.A., Sun, H., Zhao, J., and Zhao, Y. 2020. Linkages between biocrust development and water erosion and implications for erosion model implementation. Geoderma, **357**: 113973. doi:10.1016/j.geoderma.2019.113973.

Geng, Y., Ding, Y., Zhou, P., Wang, Z., Peng, C., and Li, D. 2023. Soil microbe-mediated carbon and nitrogen cycling during primary succession of biological soil crusts in tailings ponds. Sci. Total Environ. **894**: 164969. doi:10.1016/j.scitotenv.2023.164969.

Ghimire, N., Kim, B., Lee, C.M., and Oh, T.J. 2022. Comparative genome analysis among Variovorax species and genome guided aromatic compound degradation analysis emphasizing 4-hydroxybenzoate degradation in Variovorax sp. PAMC26660. BMC Genomics [Electronic Resource], **23**: 1–16. doi:10.1186/s12864-022-08589-3.

Glaser, K., Albrecht, M., Baumann, K., Overmann, J., and Sikorski, J. 2022. Biological soil crust from mesic forests promote a specific bacteria community. Front. Microbiol. **13**: 1–13. doi:10.3389/fmicb.2022.769767.

Government of Canada. 2022. Canadian climate normals 1991-2020 station data—Mont Brun, Québec [WWW Document]. Available from https://climate.weather.gc.ca/climate_normals/index_e.html [accessed 31 May 2022].

Guittonny, M., and Bussière, B. 2020. Hard rock mine reclamation. CRC Press. doi:10.1201/9781315166698.

Hammarlund, S.P., and Harcombe, W.R. 2019. Refining the stress gradient hypothesis in a microbial community. Proc. Natl. Acad. Sci. **116**: 15760–15762. doi:10.1073/pnas.1910420116.

Harris, J. 2009. Soil microbial communities and restoration ecology: facilitators or followers? Science, **325**: 573–574. doi:10.1126/science.1172975.

Haughian, S.R., and Burton, P.J. 2018. Microclimate differences above ground-layer vegetation in lichen-dominated pine forests of north-central British Columbia. Agric. For. Meteorol. **249**: 100–106. doi:10.1016/j.agrformet.2017.11.029.

Hernandez, D.J., David, A.S., Menges, E.S., Searcy, C.A., and Afkhami, M.E. 2021. Environmental stress destabilizes microbial networks. ISME J. **15**: 1722–1734. doi:10.1038/s41396-020-00882-x.

Holland-Moritz, H., Stuart, J., Lewis, L.R., Miller, S., Mack, M.C., McDaniel, S.F., and Fierer, N. 2018. Novel bacterial lineages associated with boreal moss species. Environ. Microbiol. **20**: 2625–2638. doi:10.1111/1462-2920.14288.

Holland-Moritz, H., Stuart, J.E.M., Lewis, L.R., Miller, S.N., Mack, M.C., Ponciano, J.M., et al. 2021. The bacterial communities of Alaskan mosses and their contributions to N2-fixation. Microbiome, **9**: 53. doi:10.1186/s40168-021-01001-4.

Joerg-Henrik, H. 2023. pairwise: Rasch Model Parameters by Pairwise Algorithm [WWW Document]. CRAN Contrib. Packag. doi:10.32614/CRAN.package.pairwise.

Karsten, U., Herburger, K., and Holzinger, A. 2014. Dehydration, temperature, and light tolerance in members of the aeroterrestrial green algal genus Interfilum (Streptophyta) from biogeographically different temperate soils. J. Phycol. **50**: 804–816. doi:10.1111/jpy.12210.

Keeney, D.R., and Nelson, D.W. 1982. Nitrogen—inorganic forms. *In* Methods of soil analysis: part 2 chemical and microbiological properties. *Edited by* A.L. Page, R. Miller and D.R. Keeney. American Society of Agronomy, Inc., and Soil Science Society of America, Inc. pp. 643–698. doi:10.2134/agronmonogr9.2.2ed.c33.

Kembel, S.W., Cowan, P.D., Helmus, M.R., Cornwell, W.K., Morlon, H., Ackerly, D.D., et al. 2010. Picante: R tools for integrating phylogenies and ecology. Bioinformatics, **26**: 1463–1464. doi:10.1093/bioinformatics/btq166.

Kostka, J.E., Weston, D.J., Glass, J.B., Lilleskov, E.A., Shaw, A.J., and Turetsky, M.R. 2016. The *Sphagnum* microbiome: new insights from an ancient plant lineage. New Phytol. **211**: 57–64. doi:10.1111/nph.13993.

Kulichevskaya, I.S., Suzina, N.E., Liesack, W., and Dedysh, S.N. 2010. Bryobacter aggregatus gen. nov., sp. nov., a peat-inhabiting, aerobic chemo-organotroph from subdivision 3 of the Acidobacteria. Int. J. Syst. Evol. Microbiol. **60**: 301–306. doi:10.1099/ijs.0.013250-0.

Kushkevych, I., Procházka, V., Vítězová, M., Dordević, D., Abd El-Salam, M., and Rittmann, S.K.-M.R. 2024. Anoxygenic photosynthesis with emphasis on green sulfur bacteria and a perspective for hydrogen sulfide detoxification of anoxic environments. Front. Microbiol. **15**: 1–20. doi:10.3389/fmicb.2024.1417714.

Lan, S., Wu, L., Zhang, D., and Hu, C. 2013. Assessing level of development and successional stages in biological soil crusts with biological indicators. Microb. Ecol. **66**: 394–403. doi:10.1007/s00248-013-0191-6.

Lan, S., Elliott, D.R., Chamizo, S., Felde, V.J.M.N.L., and Thomas, A.D. 2024. Editorial: biological soil crusts: spatio-temporal development and ecological functions of soil surface microbial communities across different scales. Front. Microbiol. **15**. doi:10.3389/fmicb.2024.1447058.

Langille, M.G.I., Zaneveld, J., Caporaso, J.G., McDonald, D., Knights, D., Reyes, J.A., et al. 2013. Predictive functional profiling of microbial communities using 16S rRNA marker gene sequences. Nat. Biotechnol. **31**: 814–821. doi:10.1038/nbt.2676.

Li, C., Sun, L., Jia, Z., Tang, Y., Liu, X., Zhang, J., and Müller, C. 2024. Microbial inoculants drive changes in soil and plant microbiomes and improve plant functions in abandoned mine restoration. Plant Cell Environ. 1–17. doi:10.1111/pce.15215.

Liao, K., Tao, Y., Tu, J., Zeng, Y., Li, Y., Wang, P., et al. 2024. Induced and natural moss soil crusts accelerate the C, N, and P cycles of Pb Zn tailings. Sci. Total Environ. **909**: 168657. doi:10.1016/j.scitotenv.2023.168657.

Liu, C., Cui, Y., Li, X., and Yao, M. 2021. microeco: An R package for data mining in microbial community ecology. FEMS Microbiol. Ecol. **97**: 1–9. doi:10.1093/femsec/fiaa255.

Maier, S., Tamm, A., Wu, D., Caesar, J., Grube, M., and Weber, B. 2018. Photoautotrophic organisms control microbial abundance, diversity, and physiology in different types of biological soil crusts. ISME J. **12**: 1032–1046. doi:10.1038/s41396-018-0062-8.

Mandakovic, D., Aguado-Norese, C., García-Jiménez, B., Hodar, C., Maldonado, J.E., Gaete, A., et al. 2023. Testing the stress gradient hypothesis in soil bacterial communities associated with vegetation belts in the Andean Atacama Desert. Environ. Microbiome, **18**: 24. doi:10.1186/s40793-023-00486-w.

Marusina, A., Boulygina, E., Kuznetsov, B., Tourova, T., Kravchenko, I., and Gal'chenko, V. 2001. A system of oligonucleotide primers for the amplification of nifH genes of different taxonomic groups of prokaryotes. Microbiology, **70**: 86–91. doi:10.1023/A:1004849022417.

McKnight, D., Huerlimann, R., Bower, D., Schwarzkopf, L., Alford, R., and Zenger, K. 2019. Methods for normalizing microbiome data: an ecological perspective. Methods Ecol. Evol. **10**: 389–400. doi:10.1111/2041-210X.13115.

McLeod, M.L., Bullington, L., Cleveland, C.C., Rousk, J., and Lekberg, Y. 2021. Invasive plant-derived dissolved organic matter alters microbial communities and carbon cycling in soils. Soil Biol. Biochem. **156**: 108191. doi:10.1016/j.soilbio.2021.108191.

McMurdie, P.J., and Holmes, S. 2013. Phyloseq: an R package for reproducible interactive analysis and graphics of microbiome census data. PLoS One, **8**. doi:10.1371/journal.pone.0061217.

Moreira-Grez, B., Tam, K., Cross, A.T., Yong, J.W.H., Kumaresan, D., Nevill, P., et al. 2019. The bacterial microbiome associated with arid biocrusts and the biogeochemical influence of biocrusts upon the underlying soil. Front. Microbiol. **10**: 1–13. doi:10.3389/fmicb.2019.02143.

Moynihan, M.A., and Reeder, C.F. 2023. moyn413/nifHdada2: v2.0.5. Zenodo. doi:10.5281/zenodo.3958364.

Muyzer, G., de Waal, E., and Uitterlinden, A. 1993. Profiling of complex microbial populations by denaturing gradient gel electrophoresis analysis of polymerase chain reaction-amplified genes coding for 16S rRNA. Appl. Environ. Microbiol. **59**: 695–700. doi:10.1128/aem.59.3.695-700.1993.

Nyenda, T., Jacobs, S.M., Gwenzi, W., and Muvengwi, J. 2019. Biological crusts enhance fertility and texture of gold mine tailings. Ecol. Eng. **135**: 54–60. doi:10.1016/j.ecoleng.2019.03.007.

Oh, S.-Y., Fong, J.J., Park, M.S., and Lim, Y.W. 2016. Distinctive feature of microbial communities and bacterial functional profiles in *Tricholoma matsutake* dominant soil. PLoS One, **11**: e0168573. doi:10.1371/journal.pone.0168573.

Oksanen, J., Blanchet, F.G., Friendly, M., Kindt, R., Legendre, P., Mcglinn, D., et al. 2019. Package 'vegan'.

Pepe-Ranney, C., Koechli, C., Potrafka, R., Andam, C., Eggleston, E., Garcia-Pichel, F., and Buckley, D.H. 2016. Non-cyanobacterial diazotrophs mediate dinitrogen fixation in biological soil crusts during early crust formation. ISME J. **10**: 287–298. doi:10.1038/ismej.2015.106.

Quast, C., Pruesse, E., Yilmaz, P., Gerken, J., Schweer, T., Yarza, P., et al. 2012. The SILVA ribosomal RNA gene database project: improved data processing and web-based tools. Nucleic Acids Res. **41**: D590–D596. doi:10.1093/nar/gks1219.

R Core Team. 2024. R: a language and environment for statistical computing. Found. Stat. Comput. Available from https://www.r-project.org/ [accessed 4 December 2024].

Renaudin, M., Laforest-Lapointe, I., and Bellenger, J.-P. 2022. Unraveling global and diazotrophic bacteriomes of boreal forest floor feather mosses and their environmental drivers at the ecosystem and at the plant scale in North America. Sci. Total Environ. **837**: 155761. doi:10.1016/j.scitotenv.2022.155761.

Rinehart, S., Shamir Weller, N.D., and Hawlena, D. 2022. Snail mucus increases the CO_2 efflux of biological soil crusts. Ecosystems, **25**: 537–547. doi:10.1007/s10021-021-00670-4.

Rodriguez-Caballero, E., Belnap, J., Büdel, B., Crutzen, P.J., Andreae, M.O., Pöschl, U., and Weber, B. 2018. Dryland photoautotrophic soil surface communities endangered by global change. Nat. Geosci. **11**: 185–189. doi:10.1038/s41561-018-0072-1.

Rousk, K., Jones, D.L., and DeLuca, T.H. 2013. Moss-cyanobacteria associations as biogenic sources of nitrogen in boreal forest ecosystems. Front. Microbiol. **4**: 1–10. doi:10.3389/fmicb.2013.00150.

Salazar, A., Warshan, D., Vasquez-Mejia, C., and Andrésson, Ó.S. 2022. Environmental change alters nitrogen fixation rates and microbial parameters in a subarctic biological soil crust. Oikos, **2022**: 1–12. doi:10.1111/oik.09239.

Sánchez-Cañizares, C., Jorrín, B., Poole, P.S., and Tkacz, A. 2017. Understanding the holobiont: the interdependence of plants and their microbiome. Curr. Opin. Microbiol. **38**: 188–196. doi:10.1016/j.mib.2017.07.001.

Schliep, K.P. 2011. Phangorn: phylogenetic analysis in R. Bioinformatics, **27**: 592–593. doi:10.1093/bioinformatics/btq706.

Smith, R.J., Benavides, J.C., Jovan, S., Amacher, M., and McCune, B. 2015. A rapid method for landscape assessment of carbon storage and ecosystem function in moss and lichen ground layers. Bryologist, **118**: 32. doi:10.1639/0007-2745-118.1.032.

Stuart, J., Holland-Moritz, H., Lewis, L., Jean, M., Miller, S., McDaniel, S., et al. 2021. Host identity as a driver of moss-associated N_2 fixation rates in Alaska. Ecosystems, **24**: 530–547. doi:10.1007/s10021-020-00534-3.

Su, Y., Zhao, X., Li, A., Li, X., and Huang, G. 2011. Nitrogen fixation in biological soil crusts from the Tengger desert, northern China. Eur. J. Soil Biol. **47**: 182–187. doi:10.1016/j.ejsobi.2011.04.001.

Sui, X., Li, M., Frey, B., Wang, M., Weng, X., Wang, X., et al. 2022. Climax forest has a higher soil bacterial diversity but lower soil nutrient contents than degraded forests in temperate northern China. Ecol. Evol. **12**: 1–16. doi:10.1002/ece3.9535.

Sun, X., Xu, R., Dong, Y., Li, F., Tao, W., Kong, T., et al. 2020. Investigation of the ecological roles of putative keystone taxa during tailing revegetation. Environ. Sci. Technol. **54**: 11258–11270. doi:10.1021/acs.est.0c03031.

Sun, X., Kong, T., Huang, D., Chen, Z., Zhang, Y., Häggblom, M.M., et al. 2024. Microbial sulfur and arsenic oxidation facilitate the establishment of biocrusts during reclamation of degraded mine tailings. Environ. Sci. Technol. **58**: 12441–12453. doi:10.1021/acs.est.3c10945.

Trivedi, P., Leach, J.E., Tringe, S.G., Sa, T., and Singh, B.K. 2020. Plant–microbiome interactions: from community assembly to plant health. Nat. Rev. Microbiol. **18**: 607–621. doi:10.1038/s41579-020-0412-1.

Ueda, T., Suga, Y., Yahiro, N., and Matsuguchi, T. 1995. Remarkable N_2-fixing bacterial diversity detected in rice roots by molecular evolutionary analysis of nifH gene sequences. J. Bacteriol. **177**: 1414–1417. doi:10.1128/jb.177.5.1414-1417.1995.

Vitt, D.H., Finnegan, L., and House, M. 2019. Terrestrial bryophyte and lichen responses to canopy opening in pine-moss-lichen forests. Forests, **10**: 233. doi:10.3390/f10030233.

Watson, C.D., Gardner, M.G., Hodgson, R.J., Liddicoat, C., Peddle, S.D., and Breed, M.F. 2022. Global meta-analysis shows progress towards recovery of soil microbiota following revegetation. Biol. Conserv. **272**: 109592. doi:10.1016/j.biocon.2022.109592.

Weber, B., Belnap, J., Büdel, B., Antoninka, A.J., Barger, N.N., Chaudhary, V.B., et al. 2022. What is a biocrust? A refined, contemporary definition for a broadening research community. Biol. Rev. **97**: 1768–1785. doi:10.1111/brv.12862.

Weber, B., Wu, D., Tamm, A., Ruckteschler, N., Rodríguez-Caballero, E., Steinkamp, J., et al. 2015. Biological soil crusts accelerate the nitrogen cycle through large NO and HONO emissions in drylands. Proc. Natl. Acad. Sci. **112**: 15384–15389. doi:10.1073/pnas.1515818112.

Wickham, H., and Chang, W. 2009. ggplot2: An implementation of the grammar of graphics. R package version 0.8. p. 3. Available from ht

tp://CRAN. R-project. org/package= ggplot2, 3 [accessed 4 December 2019]. doi:10.1007/978-0-387-98141-3.
Witzgall, K., Hesse, B.D., Pacay-Barrientos, N.L., Jansa, J., Seguel, O., Oses, R., et al. 2024. Soil carbon and nitrogen cycling at the atmosphere–soil interface: quantifying the responses of biocrust–soil interactions to global change. Global Change Biol. **30**: 1–18. doi:10.1111/gcb.17519.
Wright, E.S. 2016. Using DECIPHER v2.0 to analyze big biological sequence data in R. R J. **8**: 352–359. doi:10.32614/RJ-2016-025.
Wu, L., Ren, C., Jiang, H., Zhang, W., Chen, N., Zhao, X., et al. 2024. Land abandonment transforms soil microbiome stability and functional profiles in apple orchards of the Chinese Losses Plateau. Sci. Total Environ. **906**: 167556. doi:10.1016/j.scitotenv.2023.167556.
Wu, W., Ke, T., Zhou, X., Li, Q., Tao, Y., Zhang, Y., et al. 2022. Synergistic remediation of copper mine tailing sand by microalgae and fungi. Appl. Soil Ecol. **175**: 104453. doi:10.1016/j.apsoil.2022.104453.
Xue, L., Ren, H., Li, S., Leng, X., and Yao, X. 2017. Soil bacterial community structure and co-occurrence pattern during vegetation restoration in karst rocky desertification area. Front. Microbiol. **8**: 1–11. doi:10.3389/fmicb.2017.02377.
Yarberry, W. 2021. CRAN recipes: DPLYR, Stringr, Lubridate, and RegEx in R, CRAN: contributed packages. Apress, Berkeley, CA. doi:10.1007/978-1-4842-6876-6.
Yilmaz, P., Parfrey, L.W., Yarza, P., Gerken, J., Pruesse, E., Quast, C., et al. 2014. The SILVA and "All-species Living Tree Project (LTP)" taxonomic frameworks. Nucleic Acids Res. **42**: D643–D648. doi:10.1093/nar/gkt1209.
Zhang, B., Kong, W., Wu, N., and Zhang, Y. 2016. Bacterial diversity and community along the succession of biological soil crusts in the Gurbantunggut Desert, Northern China. J. Basic Microbiol. **56**: 670–679. doi:10.1002/jobm.201500751.
Zhang, L. 2024. Effects of mixed biocrusts on soil nutrients and bacterial community structure: a case study from Hilly Loess Plateau, China. Sci. Rep. **14**: 21265. doi:10.1038/s41598-024-71927-w.
Zhang, Z., Han, P., Zheng, Y., Jiao, S., Dong, H., Liang, X., et al. 2023. Spatiotemporal dynamics of bacterial taxonomic and functional profiles in estuarine intertidal soils of China coastal zone. Microb. Ecol. **85**: 383–399. doi:10.1007/s00248-022-01996-9.
Zuur, A.F., Ieno, E.N., and Elphick, C.S. 2010. A protocol for data exploration to avoid common statistical problems. Methods Ecol. Evol. **1**: 3–14. doi:10.1111/j.2041-210X.2009.00001.x.